Heliyon 10 (2024) e24353

Contents lists available at ScienceDirect

Heliyon

journal homepage: www.cell.com/heliyon

Research article

Mathematical modelling and heat transfer observations for Jeffrey nanofluid with applications of extended Fourier theory and temperature dependent thermal conductivity

D.K. Almutairi

Department of Mathematics, College of Science Al-Zulfi, Majmaah University, Al-Majmaah 11952, Saudi Arabia

ARTICLE INFO

Keywords:
Jeffrey nanofluid
Mathematical modeling
Variable thermal conductivity
Cattaneo-christov model
Stretching disks

ABSTRACT

The suspension of non-Newtonian materials with nanoparticles is important to enhance the thermal phenomenon in various engineering and industrial processes. The versatile research in nanomaterials provide different applications in thermal processes, heat exchangers, thermo-electric devices, HVAC systems, energy processes etc. Following to such novel motivations in mind, current research endorsed the enhancement in heat transfer due to suspension of Jeffrey nanofluid comprising the variable thermal conductivity. The cause of flow is associated to two disks attaining fixed distance. The modified developed relations for Fourier's hypothesis are utilized to model the problem. The flow problem is modeled with appliance of fundamental novel laws. By applying suitable transformations, corresponding differential equations are renovated into dimensionless forms which are solved with applications of analytic homotopic algorithm. The behavior of temperature and velocity due to various parameters is discussed. The numerical calculations have been done for wall shear force and Nusselt number. The results show that the velocity profile boosted due to variation of stretching ratio constant. The enhancement in heat transfer is observed due to Reynolds number. Moreover, the increasing observations for wall shear force in upper and lower disk surfaces are obtained against larger material parameter. The simulated results may find applications in improving heat transfer phenomenon, manufacturing systems, recovery processes, cooling systems, chemical phenomenon, fuel cells etc.

1. Introduction

A considerable research on non-Newtonian materials have been recently predicted by investigators due to unique rheology and distinguish consequences. The identification of nonlinear materials is subsequently discussed via nonlinear relationship. A different class of non-Newtonian materials is provoked in the literature. The Jeffrey model belong to rate type classes of non-Newtonian materials having different unique consequences. The Jeffrey material is the famous nonlinear liquid which possess the novel outcomes of retardation time and relaxation time consequences. Major applications of such liquid are observed in the polymer industries, manufacturing systems and metal industries. Referring to past studies, some contributions for Jeffrey model are presented in Refs. [1–5].

A critical role of phenomenon of heat transfer is disclosed in all engineering and industrial systems. The final outcomes of engineering and industrial framework is strictly associated to the heat transfer fluctuation. It is commonly predicted that some base liquids

E-mail address: dk.almutairi@mu.edu.sa.

https://doi.org/10.1016/j.heliyon.2024.e24353
Received 14 August 2023; Received in revised form 1 November 2023; Accepted 8 January 2024
Available online 9 January 2024

less fulfill the desired transpiration of heat transfer and subsequently effected the thermal transport phenomenon. The continuous attempts and enhancement in the thermal engineering, a new class namely nanofluid is introduced at end of last century. The nanomaterials are improved class of base liquids occupying more progressive thermal outcomes and improved heat transfer. Different nitrides, carbides, alloyed and semi-conductors are used to prepared the nanofluids. Owing to classical properties, the different applications of nanofluids are reported heating systems, engineering framework, thermal systems, transport phenomenon, refrigeration systems, heat exchangers, chemical processes, microelectronics etc. The novel primarily concept and investigation on nanofluid was firstly developed by Choi [6]. Recently some novel work on this topic has been reported by numerous scientists. Sheremet et al. [7] explored some fundamental applications of nanoparticles while performing the natural convection flow of nanofluid influenced by local heater size features. Waqas et al. [8] numerically evaluated the thermal performances in viscoelastic fluid by using nanoparticles in presence of gyrotactic microorganisms. Zaib et al. [9] specified the role of entropy generation impact while studying the thermal aspects of water-based TiO_2 nano-suspension confined by moving plate. The thermal properties of hybrid ferrofluid with additional impact of thermal radiation and external energy sources were utilized by Kumar et al. [10]. The study directed by Sheikholeslami and collaborators [11] described the thermogravitational convection phenomenon in porous chamber in presence of nanoparticles. Another investigation directed by Ma et al. [12] depicted the nanoparticles utilization in U-shaped enclosure which was additionally impact by magnetic field influences. Shahzadi and Nadeem [13] imposed the slip features for enhanced nanoparticles in porous space. The hybrid nanoparticles with influence of Lorentz force in semi annulus have been carried out in the work of Sheikholeslami et al. [14]. The research model reported by Bondarenko et al. [15] endorsed the role of heat-generating element in Al2O3/H2O nano-material in cavity. Another work performed by Mehryan et al. [16] signified the enhancement in heat transportation for nanoparticles immersed in power law nonlinear model with melting heat transfer. The third grade material confining the tiny particles under the impact of second order slip and viscous dissipation was numerically revealed by Abdelmalek et al. [17]. The work regarding slip effects expressions namely Wu's slip for Couple stress fluid flow with bioconvection definition was progressed by Khan et al. [18]. The volumetric heat transfer for nanofluid problem was computed by Oztop et al. [19]. Selimefendigil et al. [20] identified the natural convective nanofluid flow in regime of vertical cavity flow. Abbas et al. [21] observed the slip impact regarding the nanofluid due to Riga surface. Shatnawi et al. [22] discussed the Casson hybrid nanofluid thermal influence with stagnation point flow. Asmat et al. [23] claimed the interaction of nanoparticles supported by Stokes second problem. Sun et al. [24] analyzed the variable thermal impact for bio-convective flow in porous plate.

The disk flow phenomenon is novel and recently reported in many research models. For rotating disk flow, the non-Newtonian fluid flow becomes significant due to its practical and theoretical application in various areas alike medical equipment, air cleaning machines, thermal power generating system, motor rotor system and turbines etc. In fluid dynamics, rotating flow has various applications in astrophysics, geophysics and cosmology. Hayat et al. [25] deliberated MHD Jeffery fluid flow in rotating disks. Reddy et al. [26] investigated Jeffery fluid flow in oscillating disks. Flow of heat transfer in pair of stretchable rotating disks is examined by Turkyilmazoglu [27]. Khan et al. [28] successfully captured the Joule heating outcomes regarding the disk flow. The radiative analysis for Oldroyd B fluid via stretching disk was confined by Khan et al. [29]. The thermal consequences of TiO2-GO nanoparticles considered between thermally radiative disks were explored by Zangooee et al. [30]. A two exploitation of dust particles induced by rotating and stretching disk has been worked out by Turkyilmazoglu [31]. Khan et al. [32] scrutinized the mixed convection analysis for rate type fluid confined between isothermally moving disks.

The phenomenon of heat transfer is encountered a fundamental importance in various fields of biosciences and engineering. It has immense applications in the field of power generators, commercial, nuclear fusion, chemical, residential, industrial areas and especially in numerous fields of engineering. It is noticed that process of heat transfer happens due to change in temperature of body. Fourier [33] initiates the conduction law of heat which is predominately utilized long ago. Yet this law relates with gradually heat change and also acquiesces the equation of heat in parabolic form. Cattaneo [34] added time factor of thermal relaxation to modify Fourier law. The time relaxation prevail over the inconsistency of heat conduction. Christov [35] supersedes Oldroyd upper convective derivative and ordinary derivative and amended this presumption. Meraj et al. [36] used Cattaneo-Christov model of heat flux and investigated the Darcy-Forchheimer flow impact on Jeffry fluid via variable thermal conductivity. Ramesh et al. [37] discussed the diffusion-thermo aspects via modified Fourier's relation for Casson liquid. The combined study regarding the mass phenomenon and heat transport pattern convey role in the industrial framework and engineering areas such as damage of crops, air conditioning, equipment powers collectors etc. In Jeffery nanofluid, mass and heat transfer impact is investigated by Nadeem et al. [38]. Abbasi et al. [39] intended the mass transfer analysis for Jeffrey nanofluid. Hayat et al. [40] discussed the CC model for Jeffrey nanofluid flow. The process in which we measure ability of material to conduct heat is named as thermal conductivity. The material in which heat transfer in low rate is of low thermal conductivity and in material of high thermal conductivity, heat transfer in high rate. Thermal resistivity is the inverse of thermal conductivity. The thermal conductivity is classified as uniform or variable. As compared to the uniform thermal diffusivity, the fluctuation in temperature is observed in non-linear way for temperature dependent thermal conductivity. Shehzad and Abbasi [41] discussed the transfer of heat for flow of three dimensional Maxwell fluid and investigated the onsets of variable thermal conductivity for CC model. Hayat et al. [42] added the contribution for variable thermal viscosity in the Jeffrey fluid problem.

Motivated by explained investigations, aim here is develop a mathematical model for thermo-diffusion model for Jeffrey nanofluid confined between moving disks. The heat transportation model is based on modified Cattaneo-Christov expressions. Another novel aspect of current analysis is the utilization of variable thermal conductivity features. The motivations for the variable thermal are associated to different industrial and engineering applications. The HAM outcomes are observed for solving the problem. The physical demonstration of problem is observed in lower surface and upper disk layer.

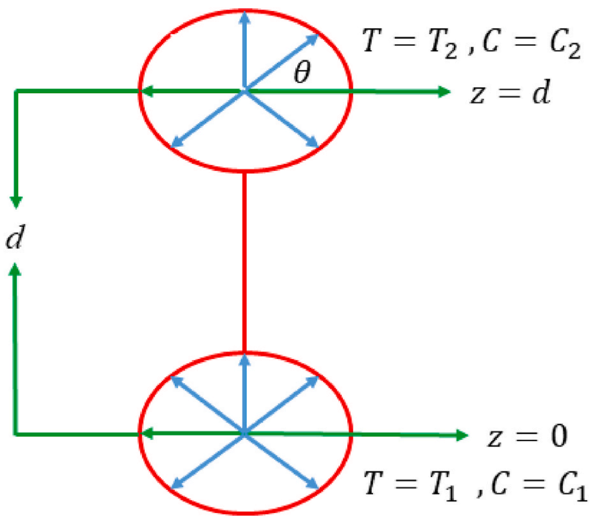

Fig. 1. Flow illustration of problem.

2. Mathematical formulation

The flow via stretched disks is considered for Jeffrey nanofluid. The disks are separated at fixed constant disks in parallel way with space $0 < z < d$. The flow is axisymmetric and steady. An opposite stretching velocities of disks causes the flow. Under the variable thermal conductivity, the inspection of heat transfer is predicted. The transverse direction magnetic force impact is considered. The mathematical modelling of problem is carried out in cylindrical coordinates (r,θ,z). The flow geometry is presented in Fig. 1. Subject to the axisymmetric constraints, the azimuthal velocity components plays no contribution. The modeled equations for formulated problem are presented as [28,29]:

$$u_r + w_z + \frac{u}{r} = 0 \tag{1}$$

$$\begin{aligned}\rho(uu_r + wu_z) = &-p_r + \frac{\mu}{1+\lambda_1}\left(u_{rr} + u_{zz} - \frac{u}{u^2} + \frac{1}{r}u_r\right)\\ &+\frac{\mu\lambda_2}{1+\lambda_1}\Bigg[u_r\left(u_{rr} - \frac{2u}{r^2}\right) + w_r u_{zr} + u\left(u_{rr} + w_{rrz} + u_{rzz} + \frac{2u}{r^3}\right)\\ &+w\left(u_{rrz} + \frac{2}{r}u_{rz} + w_{zzz} + w_{rz}\right) + u_z\left(w_{rr} + u_{rz} - \frac{2w}{r^2}\right) + w_z(u_{zz} + w_{rz}) + \frac{2}{r}u_{rr}\Bigg]\end{aligned} \tag{2}$$

$$\begin{aligned}\rho(uw_r + ww_z) = &-p_z + \frac{\mu}{1+\lambda_1}\left(w_{rr} + w_{zz} + \frac{1}{r}w_r\right)\\ &+\frac{\mu\lambda_2}{1+\lambda_1}\left[2u_{zzr} + 2u_z w_{zr} + u_r(u_{rz} + w_{rr}) + w_r u_{zz} + u(u_{rrz} + u_{rrr}) + w\left(u_{rzz} + w_{zzz} + w_{rrz} + \frac{1}{r}u_{zz} + \frac{1}{r}w_{zr}\right) + \frac{u}{r}(w_{rr} + u_{rz})\right]\end{aligned} \tag{3}$$

2.1. Cattaneo-Christov model

$$C_p\rho[T_t + (\nabla.V)T] = -\nabla.q \tag{4}$$

The velocity components u, v and w are along r, θ and z directions respectively. Furthermore, ν is being kinematic viscosity, ρ be fluid density, λ_1 is relaxation to retardation time ratio, T temperature, C_p is specific heat, λ_2 is retardation time while q is heat flux which defined as:

$$q + \lambda_H[q_t + (\nabla.V)q - q.\nabla V + V.\nabla q] = -K_f(T).\nabla T \tag{5}$$

In (5), variable thermal conductivity is $K(T)$ and time relaxation of heat flux is λ_H..
Eliminations of q yields

$$uT_r + wT_z = \frac{1}{\rho C_p}[K_f(T).T_z]_z - \lambda_H\Big[u^2T_{rr} + w^2T_{zz} + 2uwT_{rz} + (uu_r + wu_z)T_r$$

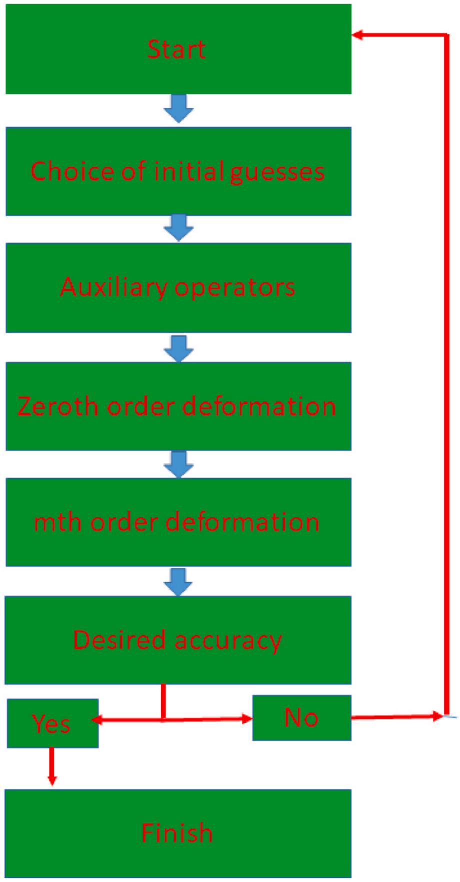

Fig. 2. Methodology chart for HAM scheme.

$$+(uw_r + ww_z)T_z] \tag{6}$$

$$uT_r + wT_z = \frac{1}{\rho C_p} K_f(T).T_{zz} + \frac{1}{\rho C_p}\left[K_f(T)\right]_z.T_z - \lambda_H \left[u^2 T_{rr} + w^2 T_{zz} + 2uwT_{rz}\right.$$

$$+(uu_r + wu_z)T_r + (uw_r + ww_z)T_z] \tag{7}$$

Replacing q by J in equation (5)

$$J + \lambda_M[J_t + (\nabla.V)J - J.\nabla V + V.\nabla J] = -D_B.\nabla T \tag{8}$$

Here J, λ_M, D_B are mass flux, time relaxation for mass flux and Brownian motion respectively.

Fick's Law is given as

$$uC_r + wC_z = D_B C_{zz} - \lambda_M\left[u^2 C_{rr} + w^2 C_{zz} + 2uwC_{rz} + (uu_r + wu_z)C_r\right.$$

$$+(uw_r + ww_z)C_z] \tag{9}$$

Boundary conditions of the problem are stated as

$$\left.\begin{array}{c} u = ar, w = 0, p = \dfrac{a\mu\beta r^2}{4d^2}, T = T_1, C = C_1 \quad \text{at } z = 0, \\ u = cr, w = 0 \quad p = 0, T = T_2, C = C_2 \quad \text{at } z = d. \end{array}\right\} \tag{10}$$

2.2. Similarity transformations

The similarity transformations for this problem are [28]:

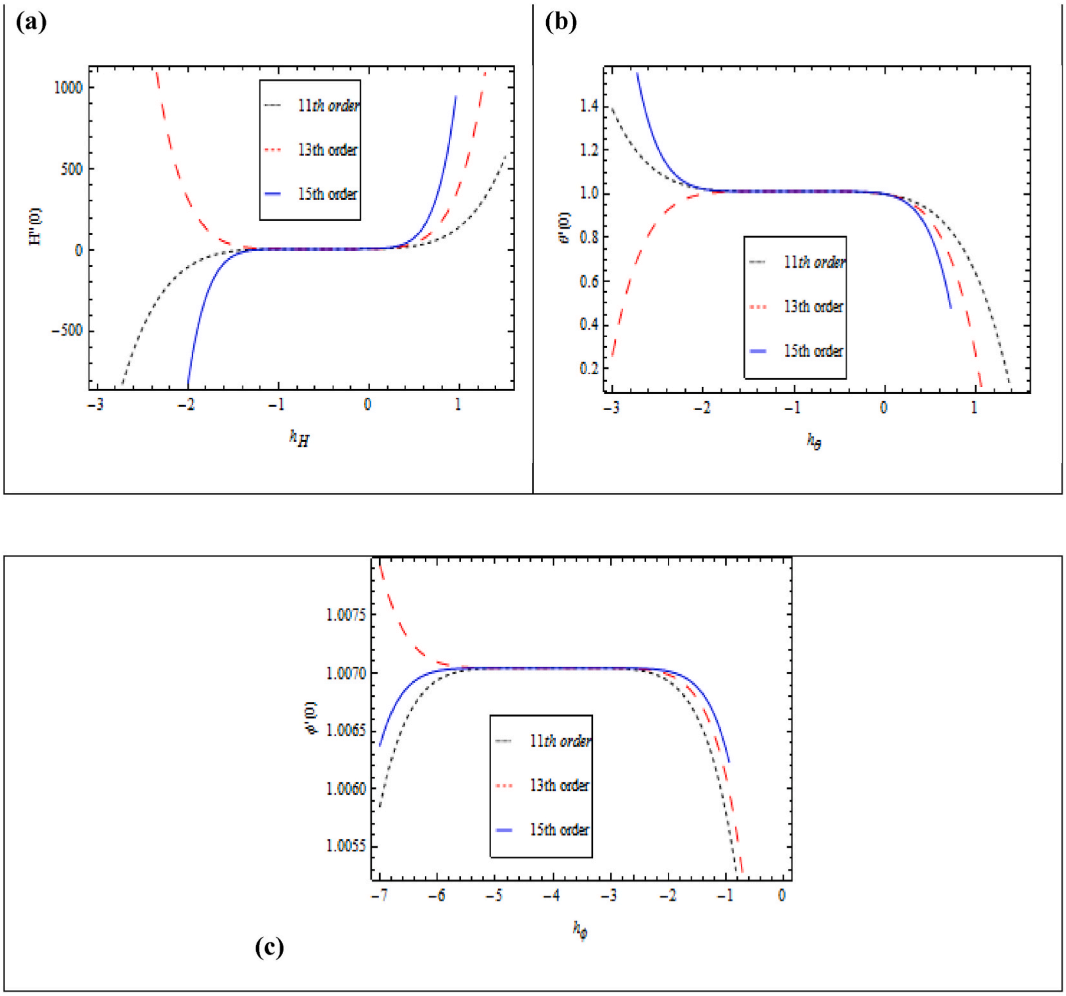

Fig. 3. *h*-curves for velocity, temperature and concentration distributions.

Table 1
The convergence analysis for HAM solution.

Order of approximation	$H^{''}(0)$	$\theta^{'}(0)$	$\varphi^{'}(0)$
3	8.14277	1.01173	1.00693
5	8.14338	1.01176	1.00703
7	8.14346	1.01176	1.00705
10	8.14346	1.01176	1.00704
15	8.14346	1.01176	1.00704

$$u = F(\eta)\text{ar}, w = H(\eta).\text{ad}, \eta = \frac{z}{d}, P = a\mu\left[p(\eta) + \frac{\beta r^2}{4d^2}\right] \tag{11}$$

$$\theta(\eta) = \frac{T_1 - T}{T_1 - T_2}, \varphi(\eta) = \frac{C_1 - C}{C_1 - C_2} \tag{12}$$

Variable thermal conductivity is stated as

$$K_f(T) = k_0\left[1 + \epsilon\left(\frac{T_1 - T}{T_1 - T_2}\right)\right] \tag{13}$$

In term of new variables, the problem of flow is modified as

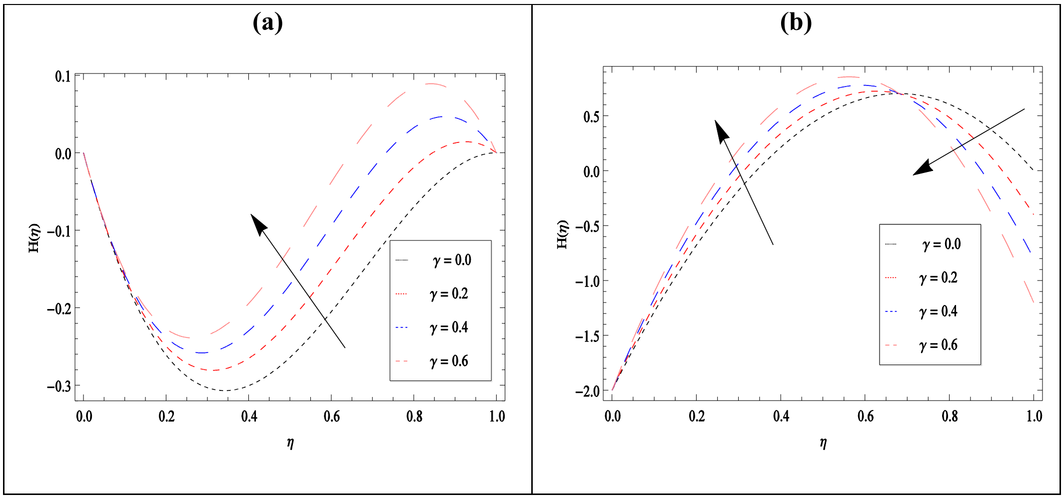

Fig. 4. Influence of γ on velocity profile when $R = 5, \lambda_2 = 0.2, \lambda_2 = 0.2$ and $\delta = 0.5$..

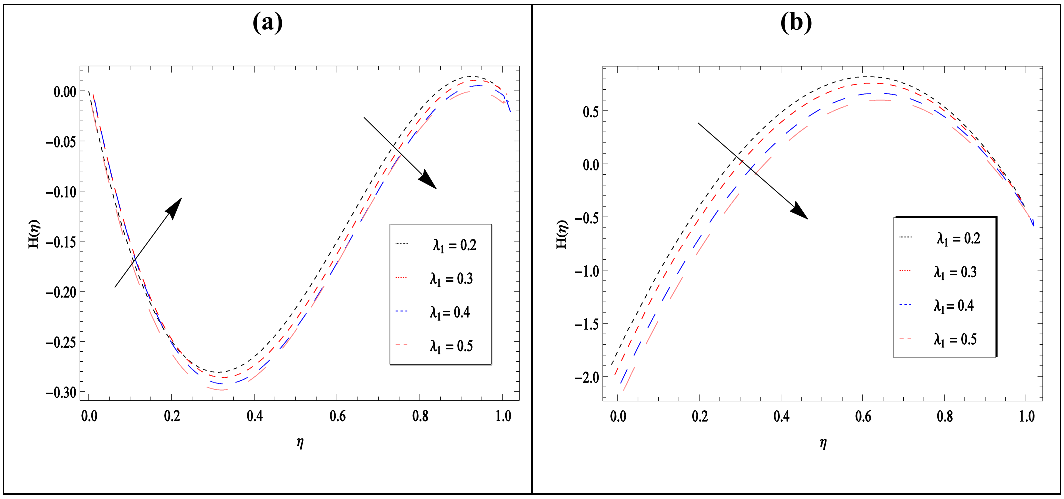

Fig. 5. Effect of λ_1 on velocity profile when $R = 5, \gamma = 0.2, h = -0.75, \lambda_2 = 0.2$ and $\delta = 0.5$..

$$2RHH''' = \frac{2}{1+\lambda_1}H^{(iv)} - \frac{\lambda_2 a}{1+\lambda_1}\left[\left(1+\frac{4}{\delta}\right)\left(HH^{(iv)} + H'H'''\right) + 2H''H'''\right] \tag{14}$$

$$RHH' = -P' + \frac{1}{1+\lambda_1}H'' + \frac{\lambda_2}{1+\lambda_1}\left(\frac{a}{2}HH'' - \frac{1}{d}H'''\right) \tag{15}$$

$$(1+\epsilon\theta)\theta'' + \epsilon\theta'^2 - \lambda_3 RHPr(H\theta'' + H'\theta') + Pr\,\theta'(Nt\theta' + Nb\varphi') - RHPr\theta' = 0 \tag{16}$$

$$\varphi'' - \lambda_4 LeRH(H\varphi'' + H'\varphi') + \frac{Nt}{Nb}\theta'' - LeRH\varphi' = 0 \tag{17}$$

with:

$$H(0) = 0, H'(0) = -2, H(1) = 0, H'(1) = -2r \tag{18}$$

$$\theta(0) = 0, \theta(1) = 1, \varphi(0) = 0, \varphi(1) = 1 \tag{19}$$

with R (Reynolds number), thermophoresis constant (Nt), material parameters (λ_1, λ_2), Hartmann number (M) , Lewis constant (Le), Brownian constant (Nb), Prandtl number (Pr) satisfying following definitions:

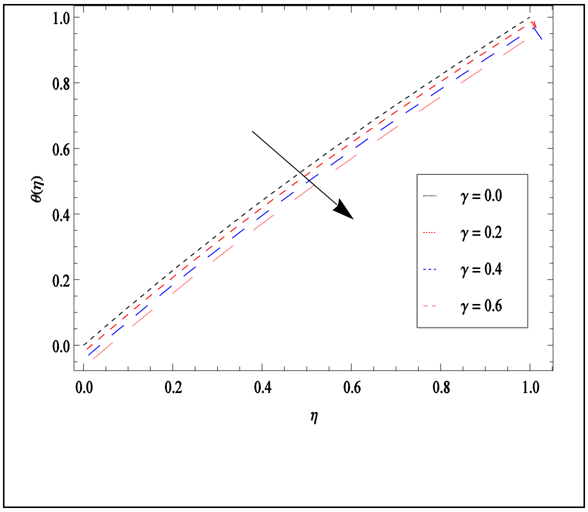

Fig. 6. Effect of γ on temperature profile.

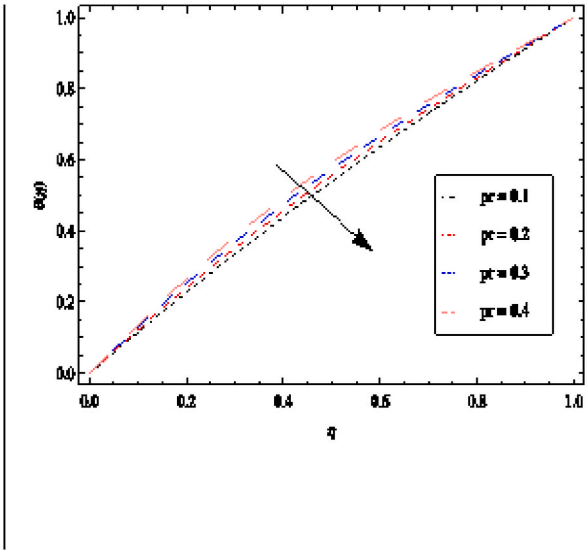

Fig. 7. Effect of *Pr* on temperature profile.

$$R = \frac{ad^2}{\nu},\ M = \frac{\sigma B_0^2}{\rho a},\ P_r = \frac{\nu}{\alpha},\ \alpha = \frac{k_0}{\rho C_p},\ \delta = \frac{r}{d},\ N_b = \tau D_B\left(\frac{C_2 - C_1}{\nu}\right),\ N_t = \frac{\tau D_T}{T_m}\left(\frac{T_2 - T_1}{\nu}\right),\ Le = \frac{\nu}{D_B},\ \lambda_3 = \lambda_H a,\ \lambda_4 = \lambda_M a.$$

2.3. *Wall shear stress*

The friction between fluid and moving fluid is called skin friction. Mathematically the skin friction is formulated as

$$C_f = \frac{\tau_w}{\frac{1}{2}\rho\nu^2}, \quad \tau_w = \tau_{rz}\big|_{z=0}, \quad \tau_w = \tau_{rz}\big|_{z=a} \tag{20}$$

where $C_{f,}\rho,\nu$ and τ_w are Coefficient of skin friction, fluid density, fluid speed and skin shear stress respectively. The lower and upper disks coefficients are:

$$C_{1f} = \frac{\tau_w}{\frac{1}{2}\rho(\delta r)^2} = \frac{\tau_{rz}\big|_{z=0}}{\frac{1}{2}\rho(\delta r)^2} = -H''(0) \tag{21}$$

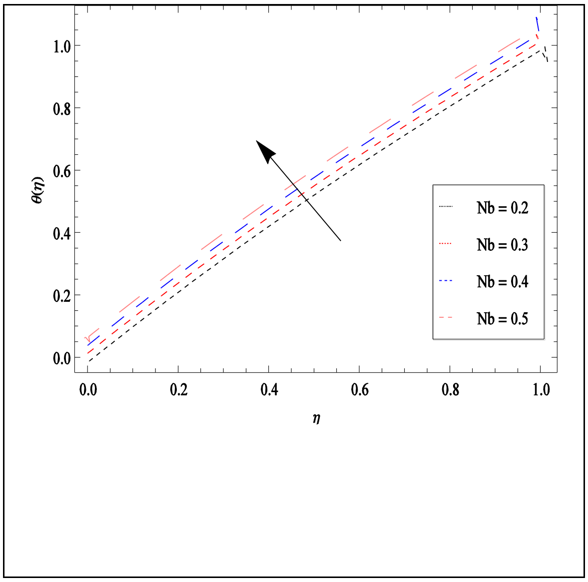

Fig. 8. Impact of *Nb* and *Nt* on temperature profile.

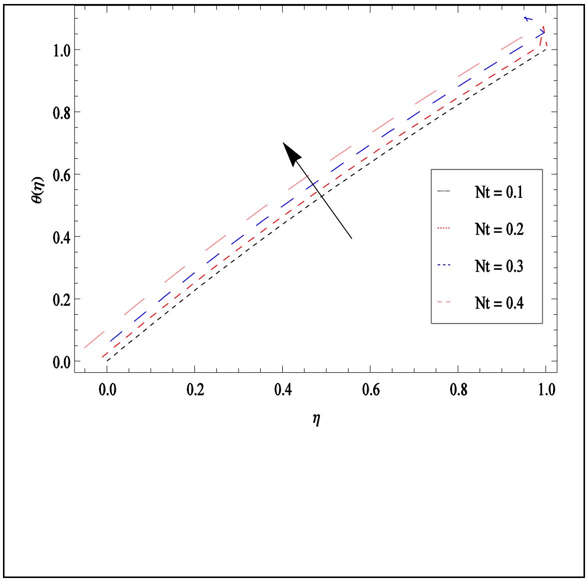

Fig. 9. Impact of *Nb* and *Nt* on temperature profile.

$$C_{2f} = \frac{\tau_w}{\frac{1}{2}\rho(\delta r)^2} = \frac{\tau_{rz}\rfloor_{z=d}}{\frac{1}{2}\rho(\delta r)^2} = -H^{''}(1) \tag{22}$$

The rate of heat transfer at surface of lower and upper disks is define as [39,40]:

$$N_{1u} = -\theta^{'}(0), \tag{23}$$

$$N_{2u} = -\theta^{'}(1). \tag{24}$$

Similarly, the dimensionless form of local Sherwood number is

$$Sh_{1u} = -\varphi^{'}(0), \tag{25}$$

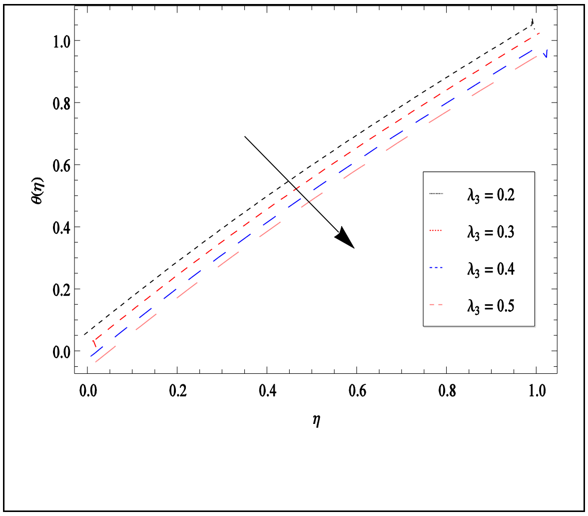

Fig. 10. Impact of λ_3 on temperature profile.

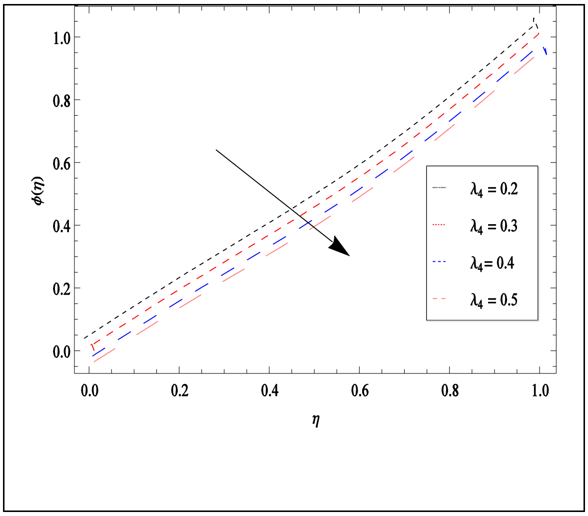

Fig. 11. Impact of λ_4 on concentration profile.

$$Sh_{2u} = -\varphi^{'}(1), \tag{26}$$

3. Solution methodology

The series solution for developed flow problem is obtained by employing homotopy scheme which is famous analytic method. This method was basically find out by Liao [43] and later on many investigations followed this procedure to simulate the desired solution [44–47]. This method is not new therefore the detail is not present here. The calculation of simulations based on HAM are summarized via Fig. 2. The convergence section is proposed in next section.

4. Convergence analysis

In HAM solution, the supporting parameters h_H, h_θ and h_φ assume an imperative part in modifying and manipulating the convergence series solution of the problem. The permissible estimations of h_H, h_θ and h_φ are often controlled by h-curves. Fig. 3 evidently demonstrates that the range for the acceptable values of $h_H \in [-0.8, 0.4]$, $h_\theta \in [-1.8, 0.4]$ and $h_\varphi \in [-5.4, 3.2]$. The optimal values of h_H, h_θ and h_φ are $h_H = -0.5$, $h_\theta = -1$ and $h_\varphi = -4.0$ additionally demonstrated by our computations. The convergence order for obtained solution in view of fixed parameters is given in Table 1. An excellent convergence at 7th order of iteration has been noticed.

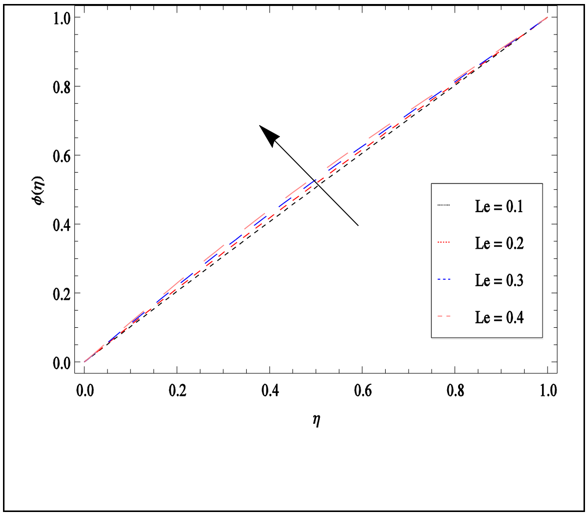

Fig. 12. Impact of *Le* on concentration profile.

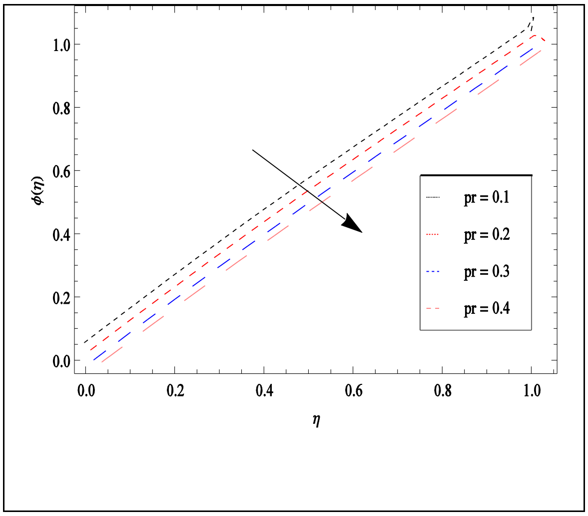

Fig. 13. Impact of *Pr* on concentration profile.

5. Discussion

The computations performed via HAM are successfully presented in previous section. The aim behind this section is to illustrates physical incorporation of parameters against the observations of physical phenomenon. The assessment is the velocity, thermal transport and concentration profile is predicted via Hartmann constant (M), stretching ratio (γ), material parameters (λ_1,λ_2), Brownian constant (Nb), Reynolds number (R), Lewis number (Le) and thermophoresis constant (Nt). After assigning variation in flow parameters, remaining parameters kept constant like $R = 5, \gamma = 0.2, \lambda_1 = 0.2, \lambda_2 = 0.2, \lambda_3 = 0.2, \lambda_4 = 0.2, Pr = 0.1, \delta = 0.5, \epsilon = 0.2, Nt = 0.1$ and $Nb = 0.5$. The variation in axial and radial velocity components for stretching ratios is γ at lower disk to upper disk, which is shown in Fig. 4(a)-(b). The axial velocity component shows progressive trend with γ. However, for radial velocity, two different observations are being noticed. The radial component shows increasing trend up to certain level and later on it decline for leading γ values. This certain change in radial component is noticed after $\eta = 0.7$. This happens because stretching velocities of walls are different. Fig. 5(a) and **(b)** discuss the significance of slip parameter λ_1 on velocity profile is shown. In Fig. 5(a), the disks are stretched and axial velocity shows decreasing behavior due to increase in λ_1. In Fig. 5(b), when λ_1 increases, the radial velocity decreases from lower disk to upper disk at definite channel then starts increasing from upper disk to lower disk. The presence of slip fluctuated the fluid velocity in both surfaces of disk. The physical description presented in Fig. 6 communicates the change in temperature θ due to γ. Lower change in lower and upper portion of disk is observed due to γ. Fig. 7 preserves the role of Pr on θ. Again, less thermal outcomes are observed for Pr. Such observations are physically referred to the less thermal diffusivity.

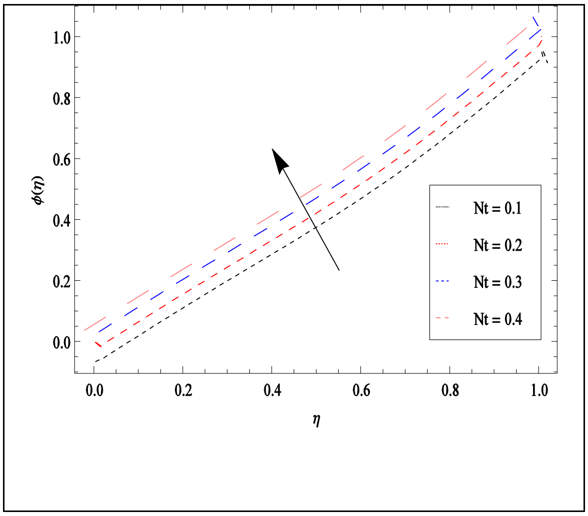

Fig. 14. Impact of *Nt* on concentration profile.

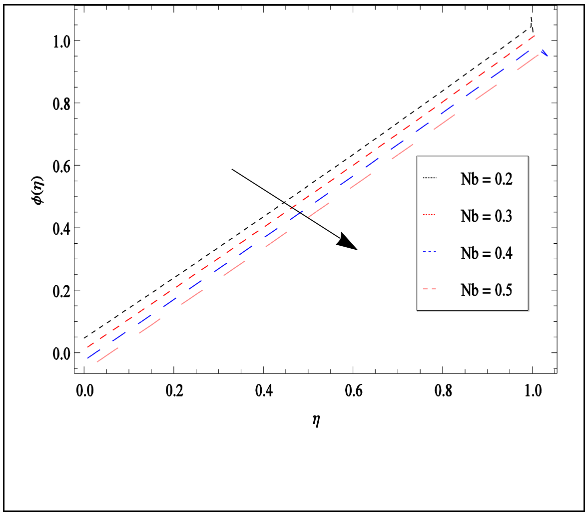

Fig. 15. Impact of *Nb* on concentration profile.

Table 2
The skin friction for various parameters at lower and upper disks.

γ	R	λ_1	λ_2	Lower disk	Upper disk
0.2				16.7261	−11.8969
0.4				18.0968	−14.9006
0.6				19.4453	−17.8036
	2.0			17.7261	−11.8951
	3.0			17.7351	−11.8931
	4.0			17.7401	−11.8821
		0.1		16.9646	−11.7952
		0.2		16.7261	−11.8961
		0.3		16.5657	−11.9601
			0.1	16.9990	−11.5945
			0.2	16.7261	−11.8961
			0.3	16.7812	−12.1048

Table 3
The variation in Nusselt number for numerous parameters at upper and lower disk.

γ	R	Pr	Nt	Nb	Lower disk	Upper disk
0.2					−1.16756	−0.870829
0.4					−1.16174	−0.878639
0.6					−1.15578	−0.886434
	2.0				−1.14057	−0.884496
	3.0				−1.14954	−0.879941
	4.0				−1.15853	−0.845386
		0.1			−1.16756	−0.870829
		0.2			−1.24358	−0.824943
		0.3			−1.32181	−0.779842
			0.1		−1.16756	−0.870829
			0.2		−1.17265	−0.867056
			0.3		−1.77770	−0.863301
				0.2	−1.15260	−0.882473
				0.4	−1.16256	−0.874701
				0.6	−1.17257	−0.866967

Fig. 8 reports the assessment of changing profile of θ with *Nb*. An enhancing trend in θ is exclusively observed with increasing *Nb*. Such increasing features are due to random fluid particles motion within disk flow. In Fig. 9, the results are claimed for illustrating change in θ against thermophoresis parameter *Nt*. The enhancement in θ is observed due to *Nt*. The increment noted due to *Nt* is referring to the thermophoresis phenomenon which is movement of fluid particles in the cooler space. The decrement in θ due to material parameters (λ_3, λ_4) and is reported from Figs. 10 and 11 in both disk surfaces. Fig. 12 accomplish the aspects of concentration profile φ with increasing values of Lewis number *Le*. The improved concentration rate is observed for larger *Le*. The aim behind presenting Fig. 13 is to identify the change in φ for Prandtl number Pr. A declining observations in the both disk surfaces is seemed due to Pr. Fig. 14 exclusively defines the change in φ for *Nt*. The concentration rate is larger for up shooting *Nt*. However, the declining assessment is noted for *Nb* against φ. < ! − −Q2 : **Fig. 15** was/were not cited in the text. Please check that the citation(s) suggested are in the appropriate place, and correct if necessary. − − > (see Fig. 15).

Table 2 is prepared in order to report the numerical values in lower and upper surface of disks when different parameters are varied. For all parameters, the variation in the lower disk is larger when compared to upper surface. The increasing impact of wall shear force is exhibited for material parameters. However, the change in numerical values in upper disk frame are very minor. Table 3 inspected the variation of Nusselt number for flow parameters. An increasing in Nusselt number is noted due to Reynolds number and stretching ratio constant.

6. Conclusions

The heat along with mass transfer mechanism due to Jeffrey nanofluid is observed under the fluctuated thermal conductivity. The extended definitions based on the Cattaneo-Christov model are used to observe the heat transfer phenomenon. The observations are predicted at both lower and upper disk surfaces. The HAM computations are performed. Major outcomes are.

- ➢ The increment in velocity from lower to upper disk is noted due to material parameter. However, reversing phenomenon is resulted in upper regime to lower surface.
- ➢ With variation of Prandtl number, the fluctuation in temperature profile has been observed from lower to upper disk.
- ➢ Due to Brownian motion, the thermal rate enhanced for Brownian constants.
- ➢ In lower disk, the mass transfer is declining due to Lewis number while reverse trend is noted in the upper disk regime.
- ➢ In lower to upper disk flow, the concentration profile enhanced with thermophoresis constant.
- ➢ The heat transfer reduces in lower disk with increasing stretching ratio constant while increasing effects are noted for Reynolds number and thermophoresis constant.
- ➢ The wall shear stress increases for upper to lower disk surface due to stretching ratio constant and material parameters.

CRediT authorship contribution statement

D.K. Almutairi: Conceptualization, Data curation, Formal analysis, Investigation, Validation, Writing - original draft, Writing - review & editing.

Declaration of competing interest

The authors declare that they have no known competing financial interests or personal relationships that could have appeared to influence the work reported in this paper.

Acknowledgment

The author extends the appreciation to the Deanship of Postgraduate Studies and Scientific Research at Majmaah University for funding this research work through the project number R-2024-927.

References

[1] Kalidas Das, Nilangshu Acharya, Prabir Kumar Kundu, Radiative flow of MHD Jeffrey fluid past a stretching sheet with surface slip and melting heat transfer, Alex. Eng. J. 54 (2015) 815–821.
[2] Sami Ullah Khan, Nasir Ali, Thermophoresis and heat generation/absorption effects on MHD flow of Jeffrey fluid over porous oscillatory stretching surface with convective boundary conditions, J. Porous Media 21 (6) (2018) 555–576.
[3] Sajjad ur-Rehman, Sohail Nadeem, Changhoon Lee, Series solution of magneto-hydrodynamic boundary layer flow over bi-directional exponentially stretching surfaces, J. Braz. Soc. Mech. Sci. Eng. 38 (2016) 443–453.
[4] B.B. Divya, G. Manjunatha, C. Rajashekhar, Vaidya Hanumesh, K.V. Prasad, The hemodynamics of variable liquid properties on the MHD peristaltic mechanism of Jeffrey fluid with heat and mass transfer, Alex. Eng. J. 59 (2) (March 2020) 693–706.
[5] Azhar Ehtsham, E.N.Maraj Z.Iqbal, Viscous dissipation performance on stagnation point flow of Jeffrey fluid inspired by internal heat generation and chemical reaction, Therm. Sci. Eng. Prog. 13 (October 2019) 100377.
[6] S.U.S. Choi, Enhancing thermal conductivity of fluids with nanoparticles, ASME Pub. Fed. 231 (1995) 99–106.
[7] A. Mikhail, Sheremet, Ioan Pop, Effect of local heater size and position on natural convection in a tilted nanofluid porous cavity using LTNE and Buongiorno's models, J. Mol. Liq. 266 (15 September) (2018) 19–28.
[8] Waqas Hassan, Sami Ullah Khan, Iskander Tlili, Muhammad Awais, Mostafa S. Shadloo, Significance of bioconvective and thermally dissipation flow of viscoelastic nanoparticles with activation energy features: novel biofuels significance, Symmetry 12 (2) (2020) 214.
[9] Aurang Zaib, Rizwan Ul Haq, Mohsen Sheikholeslami, Ali J. Chamkha, Mohammad Mehdi Rashidi, Impact of non-Darcy medium on mixed convective flow towards a plate containing micropolar water-based TiO_2 nanomaterial with entropy generation, J. Porous Media 23 (1) (2020) 11–26.
[10] K. Anantha Kumar, N. Sandeep, V. Sugunamma, I.L. Animasaun, Effect of irregular heat source/sink on the radiative thin film flow of MHD hybrid ferrofluid, J. Therm. Anal. Calorim. 139 (2020) 2145, https://doi.org/10.1007/s10973-019-08628-4.
[11] M. Sheikholeslami, A.Sheremet Mikhail, Shafee Ahmad, Tlili Iskander, Simulation of nanoliquid thermogravitational convection within a porous chamber imposing magnetic and radiation impacts, Phys. Stat. Mech. Appl. (2020) 124058.
[12] Ma Yuan, Mohebbi Rasul, M.M. Rashidi, Yang Zhigang, Mikhail A. Sheremet, Numerical study of MHD nanofluid natural convection in a baffled U-shaped enclosure, Int. J. Heat Mass Tran. 130 (March 2019) 123–134.
[13] I. Shahzadi, S. Nadeem, Impinging of metallic nanoparticles along with the slip effects through a porous medium with MHD, J. Braz. Soc. Mech. Sci. Eng. 39 (2017) 2535.
[14] M. Sheikholeslami, H. Öztop, N. Abu-Hamdeh, Z. Li, Nanoparticle transportation of CuO-H_2O nanofluid in a porous semi annulus due to Lorentz forces, Int. J. Numer. Methods Heat Fluid Flow 29 (1) (2019) 294–308.
[15] Darya S. Bondarenko, A. Sheremet Mikhail, F.Oztop Hakan, E.Ali Mohamed, Natural convection of Al2O3/H2O nanofluid in a cavity with a heat-generating element. Heatline visualization, Int. J. Heat Mass Tran. 130 (March 2019) 564–574.
[16] S.A.M. Mehryan, Vaezi Mohammad, Sheremet Mikhail, Ghalambaz Mohammad, Melting heat transfer of power-law non-Newtonian phase change nano-enhanced n-octadecane-mesoporous silica (MPSiO2), Int. J. Heat Mass Tran. 151 (April 2020) 119385.
[17] Zahra Abdelmalek, Sami Ullah Khan, Waqas Hassan, Hossam A. Nabwey, Iskander Tlili, Utilization of second order slip, activation energy and viscous dissipation consequences in thermally developed flow of third grade nanofluid with gyrotactic microorganisms, Symmetry 12 (2) (2020) 309.
[18] Sami Ullah Khan, H. Waqas, M.M. Bhatti, M. Imran, Bioconvection in the rheology of magnetized Couple stress nanofluid featuring activation energy and Wu's slip, J. Non-Equilibrium Thermodyn. 45 (1) (2020) 81–95.
[19] F.Oztop Hakan, Eiyad Abu-Nada, Ali Chamkha YasinVarol, Natural convection in wavy enclosures with volumetric heat sources, Int. J. Therm. Sci. 50 (4) (April 2011) 502–514.
[20] Fatih Selimefendigil, F. Oztop Hakan, Ali J. Chamkha, MHD mixed convection in a nanofluid filled vertical lid-driven cavity having a flexible fin attached to its upper wall, J. Therm. Anal. Calorim. 135 (2019) 325–340.
[21] N. Abbas, W. Shatanawi, K.U. Rehman, T.A. Shatnawi, Velocity and thermal slips impact on boundary layer flow of micropolar nanofluid over a vertical nonlinear stretched Riga sheet, Proc. Inst. Mech. Eng., Part N: Journal of Nanomaterials, Nanoengineering and Nanosystems (2023) 23977914231156685.
[22] T.A. Shatnawi, N. Abbas, W. Shatanawi, Mathematical analysis of unsteady stagnation point flow of radiative Casson hybrid nanofluid flow over a vertical Riga sheet, Mathematics 10 (19) (2022) 3573.
[23] F. Asmat, W.A. Khan, I. Khan, T. Muhammad, A scientific report on Stokes' second problem for a transient nanofluid model with a heated boundary in the presence of a magnetic field, J. Magn. Magn Mater. 586 (2023) 171171.
[24] S. Sun, S. Li, S. Shaheen, M.B. Arain, Usman, K.A. Khan, A numerical investigation of bio-convective electrically conducting water-based nanofluid flow on the porous plate with variable wall temperature, Numer. Heat Tran., Part A: Applications (2023) 1–15.
[25] T. Hayat, M. Nawaz, M. Awais, S. Obaidat, Axisymmetric magnetohydrodynamic flow of Jeffrey fluid over a rotating disk, Int J Numer Methods Fluids 70 (6) (2012) 764–774.
[26] G.B. Reddy, S. Sreenadh, R.H. Reddy, A. Kavitha, Flow of a Jeffrey fluid between torsionally oscillating disks, Ain Shams Eng. J. 6 (2015) 355–362.
[27] M. Turkyilmazoglu, Flow and heat simultaneously induced by two stretchable rotating disks, Phys. Fluids 28 (2016) 043601.
[28] N. Khan, M. Sajid, T. Mahmood, Heat transfer analysis for magnetohydrodynamicsaxi-symmetric flow between stretching disks in the presence of viscous dissipation and joule heating, AIP Adv. 5 (2015) 057115.
[29] N. Khan, T. Mahmood, Thermophoresis particle deposition and internal heat generation on MHD flow of an Oldroyd-B nanofluid between radiative stretching disks, J. Mol. Liq. 216 (2016) 571–582.
[30] M.R. Zangooee, Kh Hosseinzadeh, D.D. Ganji, Hydrothermal analysis of MHD nanofluid (TiO2-GO) flow between two radiative stretchable rotating disks using AGM, Case Stud. Therm. Eng. 14 (2019) 100460. Article.
[31] M. Turkyilmazoglu, Suspension of dust particles over a stretchable rotating disk and two-phase heat transfer, Int. J. Multiphas. Flow 127 (2020) 103260. Article.
[32] Nargis Khan, A. Hossam, Nabwey, muhammad sadiq hashmi, Sami ullah khan and iskander tlili, A theoretical analysis for mixed convection flow of Maxwell fluid between two infinite isothermal stretching disks with heat source/sink, Symmetry 12 (2020) 62, https://doi.org/10.3390/sym12010062.
[33] Fourier Jbj, ThéorieAnalytique De La Chaleur, 1822. Paris.
[34] C. Cattaneo, Sulla conduzione del calore, AttiSemin Mat FisUniv Modena Reggio Emilia 3 (1948) 83–101.
[35] C.I. Christov, On frame indifferent formulation of the Maxwell-Cattaneo model of finite-speed heat conduction, Mech. Res. Commun. 36 (2009) 481–486.
[36] M.A. Meraj, S.A. Shehzad, T. Hayat, F.M. Abbasi, A. Alsaedi, Darcy-Forchheimer flow of variable conductivity Jeffrey liquid with Cattaneo-Christov heat flux theory, Appl. Math. Mech. 38 (4) (2017) 557–566.
[37] G.K. Ramesh, B.J. Gireesha, S.A. Shehzad, F.M. Abbasi, Analysis of heat transfer phenomenon in MagnetohydrodynamicCasson fluid flow through Cattaneo-Christov heat diffusion theory, Commun. Theor. Phys. 68 (1) (2017).
[38] S. Nadeem, N.S. Akbar, Influence of haet and mass transfer on a peristaltic motion of a Jeffrey-six constant fluid in an annulus, Heat Mass Transf 46 (2010) 485–493.

[39] F.M. Abbasi, S.A. Shehzad, T. Hayat, A. Alsaedi, M.A. Obid, Influence of heat and mass flux conditions in hydromagnetic flow of Jeffreynanofluid, AIP Adv. 5 (2015) 037111.

[40] T. Hayat, S. Qayyum, S.A. Shehzad, A. Alsaedi, Cattaneo-Christove double diffusion model for flow of Jeffrey fluid, J. Braz. Soc. Mech. Sci. Eng. 1–17 (2017), https://doi.org/10.1007/s40430-017-0793-x.

[41] F.M. Abbasi, S.A. Shehzad, Heat transfer analysis for three dimensional flow of Maxwell fluid with temperature dependent thermal condutivity: application of Cattaneo-Christov heat flux model, J. Mol. Liq. 220 (2016) 848–854.

[42] T. Hayat, S.A. Shehzad, A. Alsaedi, Three-dimensional stretched flow of Jeffery fluid with variable thermal conductivity and thermal radiation, Appl. Math. Mech. 34 (2013) 823–832.

[43] S.J. Liao, Advances in the Homotopy Analysis Method, World Scientific Publishing, 5 Toh Tuck Link, Singapore, 2014.

[44] M. Turkyilmazoglu, Analytic approximate solutions of rotating disk boundary layer flow subject to a uniform suction or injection, Int. J. Mech. Sci. 52 (2010) 1735–1744.

[45] M. Turkyilmazoglu, The analytical solution of mixed convection heat transfer and fluid flow of a MHD viscoelastic fluid over a permeable stretching surface, Int. J. Mech. Sci. 77 (2013) 263–268.

[46] Sami Ullah, A Rauf Khan, Sabir Ali Shehzad, Z. Abbas, T. Javed, Study of bioconvection flow in Oldroyd-B nanofluid with motile organisms and effective Prandtl approach, Phys. Stat. Mech. Appl. 527 (2019). Article No. 121179.

[47] Sami Ullah Khan, Sabir Ali Shehzad, Brownian movement and thermophoretic aspects in third grade nanofluid over oscillatory moving sheet, Phys. Scripta 94 (9) (2019) 095202.